



Modular microfluidic reactor and inline filtration system for the biocatalytic synthesis of chiral metabolites

Brian O'Sullivan^a, Homam Al-Bahrani^a, James Lawrence^a, Maria Campos^a, Armando Cázares^b, Frank Baganz^a, Roland Wohlgemuth^c, Helen C. Hailes^b, Nicolas Szita^{a,*}

^a Department of Biochemical Engineering, University College London, Torrington Place, London WC1E 7JE, UK

^b Department of Chemistry, University College London, 20 Gordon Street, London WC1H 0AJ, UK

^c Sigma-Aldrich, Industriestrasse 25, 9470 Buchs, Switzerland

ARTICLE INFO

Article history:

Received 9 August 2011

Received in revised form 1 December 2011

Accepted 30 December 2011

Available online 8 January 2012

Keywords:

Microfluidic reactor

Filtration

Transketolase

Chiral metabolites

Bioprocess microfluidics

Microfluidic downstream processing

ABSTRACT

Biocatalytic synthesis is now well established amongst catalytic methodologies as an extremely useful approach for the industrial synthesis of high-value compounds, due to its many advantages such as high reaction specificity and selectivity. However, engineering a biocatalytic process can be complex and time-consuming. This paper presents a modular microfluidic reactor and in-line filtration system for the rapid and small-scale evaluation of biocatalytic reactions. The system combines a substrate with a biocatalyst in free solution, incubates the two components until full conversion to product has been achieved, before extracting the product. The system has been applied to the transketolase-catalysed reaction of hydroxypyruvate (HPA) and glycolaldehyde (GA) to L-erythrose, demonstrating complete conversion of substrate to product, complete retention of the enzyme and an overall yield of approximately 65%. The complete conversion of HPA and propanal to (3S)-1,3-dihydroxypentan-2-one with a mutant transketolase further demonstrated the applicability of the microfluidic system for organic synthesis.

© 2012 Elsevier B.V. All rights reserved.

1. Introduction

Inspired by the rapid advances and successes of microfluidic reactors for chemical synthesis [1] and underpinned by the development of microfluidic enzyme reactors as analytical tools for proteomic studies [2], several groups have begun to develop and explore the use of microfluidic reactors in the field of biochemical synthesis [3–9]. Many advantages have been reported with the use of microfluidic reactors, including more precise control over reaction conditions, real time monitoring of reaction efficiency, more effective thermal transfer due to larger surface area to volume ratios, reduced use of resources, and an increased throughput via parallelisation [1,10]. These advantages can potentially enable the rapid evaluation of different reaction conditions, overcoming the time constraints typically associated with biocatalytic process development. However, for real implementation in industrial settings it will be necessary to embed the reaction (upstream) steps with separation and purification (downstream) steps to enable continuous synthesis and isolation of pharmaceutical intermediates or metabolites. For chemical

synthesis and work-up, the power of modular networks consisting of microfluidic reactor and separator units that can easily be arranged into different configurations has already been shown [11,12]. We want to demonstrate that microfluidic devices can equally provide a modular toolbox for the development of whole biocatalytic processes, i.e. for both the upstream and downstream unit operations.

The impact of process integration (i.e. the integration of a biocatalytic reaction with the subsequent separation and purification steps) for efficient product recovery and process intensification has already been shown in conventional reactors [13,14]. In batch as well as in continuous-flow systems, there is a need for the separation of the biocatalyst and the product, either to retain the biocatalyst for reuse, to purify the product or to quench the reaction (in the case of kinetic studies). This can be achieved either by immobilisation of the biocatalyst or by ultrafiltration (typically in tangential or cross-flow filtration mode), separating the high-molecular weight biocatalyst from the desired low-molecular weight product. A variety of biocatalyst immobilisation methods on solid supports as well as biocatalyst crosslinking methods have been described for use in microfluidic reactors [5,7,10,15–20]. Whilst immobilisation may improve the stability of the biocatalyst, it adds further complexity to the fabrication and reduces the flexibility of easy-to-use microfluidic reactors. On the other hand,

* Corresponding author. Tel.: +44 020 7679 4418; fax: +44 020 7916 3943.

E-mail address: n.szita@ucl.ac.uk (N. Szita).

membrane separation processes for ultrafiltration are well established downstream operations in industrial production processes towards the recovery of products [21], and simple 'clamp-and-play' type devices for the integration of membranes into microfluidic systems have previously been established [22].

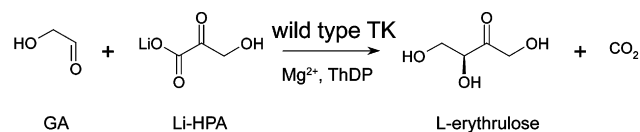
A loop/recirculation microfluidic enzyme reactor integrated with a regenerated cellulose membrane for separation of low-molecular weight pectin hydrolysates from high-molecular weight pectin has recently been developed [8]. In this configuration, the membrane was integrated together with the reactor. This integrated configuration has been useful when applied to high-molecular weight pectin substrates, where the product removal occurs due to the large molecular weight difference between the pectin substrate and the low-molecular weight pectin fragments (product). However, such an integrated configuration is not directly applicable to the vast number of biocatalytic reactions involving transformations of low-molecular weight substrates. These substrates would pass through the membrane before they were converted to product. We therefore sought to engineer a system which would work with low-molecular weight substrates and where the design of the microfluidic system would allow for the individual optimisation of the reaction and separation parameters.

For the efficient separation of high-molecular weight enzymes from the desired low-molecular weight product, the filtration method has to be robust, compatible with the microreactor and resistant to fouling. Tangential flow regimes are preferable as they help prevent the build up of macromolecules on the membrane surface [23,24]. This should allow the system to be operated for a longer period of time without changing or cleaning the membrane, as well as reducing the amount of biocatalyst lost in the process. In tangential flow systems, the transmembrane pressure is a crucial parameter for successful operation. It is therefore desirable to be able to test different membranes and operating conditions for the tangential flow filtration independent from the reaction conditions.

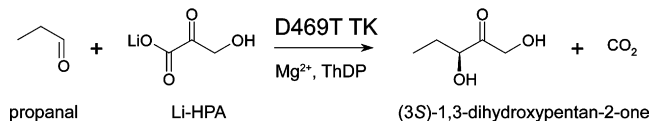
The optimisation of the reaction parameters in the microfluidic reactor requires a well-defined biotransformation yielding a single product. We have selected the transketolase-catalysed two-carbon addition of hydroxypyruvate to glycolaldehyde and propanal. Transketolases have been shown to be attractive biocatalysts in the asymmetric synthesis of chiral metabolites [25–30] with a wide substrate tolerance and high specificity of product formation. The use of hydroxypyruvate enables the formation of new carbon–carbon bonds with excellent enantioselectivity and allows the reaction to go to completion because of the release of carbon dioxide. The coupling of transketolase reactions with either a subsequent transaminase reaction [31] or a preceding triosephosphate isomerase reaction [32] has on one hand already demonstrated the opportunities for combining the transketolase reaction step with other reaction steps, but has on the other hand also shown the importance of a good selection and control of the reaction parameters due to instabilities of reactants.

In this work, a modular microfluidic reactor and a tangential flow filtration system have been used with the enzyme transketolase (TK) to produce a chiral metabolite, L-erythrulose (Reaction A, Scheme 1), and to subsequently separate this metabolite from the biocatalyst, transketolase, producing two distinct outputs – a purified product solution and a concentrated catalyst solution. We investigated the conditions required to obtain full conversion and separation of the product. The system was further used with a more hydrophobic substrate, propanal, to give (3S)-1,3-dihydroxypentan-2-one (DHP) (Reaction B). To our knowledge, this is the first study to combine metabolite synthesis using a biocatalyst in solution with an inline separation step on a microfluidic platform.

Reaction A



Reaction B



Scheme 1. Two transketolase-catalysed reactions studied in this research: the formation of L-erythrulose from glycolaldehyde (A), and the formation of DHP from propanal (B).

2. Materials and methods

2.1. Reagents and analysis

Unless otherwise stated, all chemicals and reagents (Sigma–Aldrich, Gillingham, UK) were used without further purification. For HPLC calibration standards, commercially available L-erythrulose was purified by flash silica chromatography as described by Smith et al. [33].

Protein concentrations were measured by SDS–PAGE electrophoresis with 12% Tris–glycine resolving gel, using purified TK standards. 20 μg of total protein was applied to each lane and the samples were stained with Coomassie Blue R-250.

HPLC analysis of products from transketolase-catalysed reactions was performed on an Aminex (Biorad, Hemel Hempstead, UK) ion-exchange column (HPX-87H, 300 mm × 7.8 mm), mobile phase: 0.1% (v/v) aqueous trifluoroacetic acid (TFA) at 0.6 mL min^{−1}. HPA and L-erythrulose were quantified from calibration curves of standard solutions, and detected by UV absorption at 210 nm.

Enantiomeric excess data for the formation of L-erythrulose were calculated from chiral HPLC analysis of the derivatised ketodiols compared to racemic standards [33,34]. The enantiomeric excess for (3S)-1,3-dihydroxypentan-2-one was obtained by derivatisation and chiral HPLC [26].

2.2. Fabrication of microfluidic components

The enzymatic microfluidic reactor and the rigid parts of the filtration unit were machined from poly(methylmethacrylate) (PMMA) with a micromilling machine (Folken IND, Glendale, USA). Microreactor PMMA components were sealed by thermal bonding (1.5 h, 105 °C).

Gaskets for the filtration unit were made from poly(dimethylsiloxane) (PDMS, Sylgard 184, Dow Corning, Midland, USA), prepared according to the manufacturer's instructions and cast in PMMA moulds which had been machined as described above.

Membranes for the filtration unit were cut to size from commercially available regenerated cellulose sheets (Durapore, Millipore, Cork, Ireland) using a CO₂ laser marking head (Synrad Inc., Mukilteo, WA, USA). The molecular weight cut-off of the membrane was 10 kDa.

Interconnect ports were milled from 5 mm PMMA, with two holes tapped with an M3 thread for attachment to the device, and an M6 threaded hole to allow standard connection fittings to be used (P-221, Upchurch Scientific, Oak Harbor, WA, USA). A more detailed description of the fabrication can be found in the [Electronic Supplementary Information \(ESI 1\)](#).

2.3. Staggered herringbone mixer studies

Two solutions (reverse-osmosis purified water and fluorescein-conjugated bovine serum albumin in phosphate buffered saline, pH 7) were flowed through separate inlet ports of two microreactors of identical dimensions, one with a passive mixer, one without. Images were taken at 10 \times magnification using a microscope fitted with a CCD camera under fluorescent light with a FITC filter (Nikon Instruments Europe B.V., Kingston, UK).

2.4. Preparation of transketolase lysate

Transketolase lysates were prepared according to the method of Matosevic et al. [35]. For the wild type TK, overnight cultures of *Escherichia coli* BL21gold(DE3) (with transketolase-producing plasmid pQR791) were grown in 200 mL shake-flasks from inoculation of 20 mL Lysogeny Broth (LB)–glycerol with a single colony obtained by streaking out cells from glycerol stocks (25%, v/v, glycerol stored at -80°C) on (LB)–agar plates. This was incubated for 12–16 h at 37°C . The resulting cell suspension was transferred to a conical flask with 200 mL LB–glycerol medium, which was incubated at 37°C until the bacterial growth had reached stationary phase, as confirmed by optical density measurements. The contents of the flask were transferred to 50 mL falcon tubes and centrifuged at 5000 rpm for 10 min. The supernatant was discarded and the cell paste was frozen at -80°C until needed for lysis and purification.

For lysis, the cell paste was resuspended in 5 mL 50 mM Tris buffer, cooled on ice and sonicated (10 cycles of 10 s on, 10 s off) with a sonication probe (Soniprep 150, Sanyo, Japan). The suspension was then centrifuged and filtered with a 0.2 μm filter, and stored at -80°C until required.

For the mutant D469T TK, the same procedure was followed except the pQR791 plasmid had been specifically mutated according to the methods of Hibbert et al. [27,28].

2.5. Batch transketolase reaction

For the reaction of HPA with glycolaldehyde, 30 μL wild type TK lysate (4.47 mg mL^{-1}) was incubated with 170 μL cofactor solution (23.1 mM MgCl_2 , 5.7 mM thiamine diphosphate in 50 mM Tris–HCl buffer, pH 7) for 20 min at room temperature. 150 μL of this solution was added to 150 μL substrate solution (100 mM hydroxypyruvate, 100 mM glycolaldehyde in 50 mM Tris–HCl buffer, pH 7) in a 96-well plate to initiate the reaction (final concentrations: 50 mM HPA, 50 mM GA, 0.34 mg mL^{-1} wild type TK, 2.4 mM ThDP, 9.8 mM MgCl_2). Aliquots (20 μL) were removed at the required time intervals, quenched with 180 μL 0.1% (v/v) aqueous TFA, centrifuged (5000 rpm, 5 min) and the supernatant analysed by HPLC.

The same protocol was used for the mutant TK-catalysed reaction of HPA with propanal (final reaction conditions: 50 mM HPA, 70 mM PA, 0.33 mg mL^{-1} TK mutant D469T, 2.4 mM ThDP, 9.8 mM MgCl_2 , room temperature, pH 7).

2.6. Continuous flow microfluidic transketolase reaction

TK lysate solutions and substrate solutions were prepared at the concentrations described above. Using a twin syringe drive, the solutions were pumped into separate inlets of the microfluidic reactor at the same flow rate for at least 1.5 times the residence time before collecting the output in pre-weighed sample vials containing 400 μL 0.1% TFA. The quenched reaction mixture was centrifuged and analysed by HPLC as above. Residence times were calculated by dividing the reactor volume (60 μL) by the flow rate.

2.7. Filtration: back pressure measurements

Constricting capillaries (internal diameter 50, 75, 100 and 200 μm) were attached to the retentate outlet of the filtration device in cross-flow mode (Fig. 2D). The resulting back pressure was measured with an inline pressure sensor (40PC100, Honeywell, NJ, USA), and the data logged with a simple LabVIEW instrument (National Instruments, TX, USA).

2.8. Filtration: proof of concept

The filtration unit was charged with Tris buffer (50 mM, pH 7). A model stock solution of TK (0.22 mg mL^{-1}) and L-erythrose (50 mM) in Tris buffer (50 mM, pH 7) was pumped through the retentate inlet with a syringe drive, whilst Tris buffer was pumped through the permeate inlet. Samples were collected at the retentate and permeate outlets for analysis by HPLC and SDS–PAGE.

For the integration of the microfluidic reactor and the filtration unit, a hydroxypyruvate/glycolaldehyde solution (both 100 mM) and a TK/cofactors solution (0.68 mg mL^{-1} TK) were combined and flowed through a microfluidic reactor at $10\text{ }\mu\text{L min}^{-1}$. Final reagent and enzyme concentrations were identical to the batch reaction conditions in Section 2.5. The output was connected to a filtration unit via a length of tubing to give the desired residence time. A 50 μm i.d. capillary was fitted to the retentate outlet of the filtration unit. The reaction was run for a total of 10 h. Samples taken from the retentate and permeate outlets were analysed by HPLC.

3. Results and discussion

3.1. Design considerations for the modular microfluidic system

3.1.1. Enzymatic continuous flow microfluidic reactor

In previous work, an immobilised enzyme microreactor for quantitative kinetic analysis of TK-catalysed reactions [16] was developed. Whilst this microreactor enables the rapid quantification of enzyme kinetic parameters, achieving complete substrate conversion with this microreactor is difficult. For biocatalytic process development, however, it is desirable to quickly achieve complete substrate conversion, and to have a tool that enables the rapid evaluation of the reaction conditions that lead to complete conversion. We therefore investigated the use of a microfluidic reactor with solubilised enzymes, where complete conversion with carbon–carbon bond forming enzymes has previously been reported [9]. Similar to this and other solubilised enzyme reactors, in our microfluidic reactor enzyme and substrate are co-flowed through a T-channel. The residence time is determined by the combined flow rate of the substrate and enzyme solution, and different reaction conditions are obtained by altering the individual flow rates and the concentrations. In contrast to other microfluidic reactors, we used wider and deeper channels (width 500 μm , depth 250 μm , length 89.5 mm, Fig. 1A). These larger structures significantly reduce the long transition times that typically occur in very shallow channels when the flow rate is changed [36]. Shortened transition times translate to less 'dead' time during the evaluation of different reaction conditions where the flow rate is frequently changed. Additionally, by using slightly larger channel structures, it was possible to machine both the reactor and filtration unit from the same material, and with the same fabrication technology. This unified approach will simplify further integration of the reactor and separator units into easily configurable modular synthesis networks.

To make valid comparisons between the kinetics of the microfluidic reactor and those of the batch, it is essential that the reagents are thoroughly mixed very quickly after being brought together.

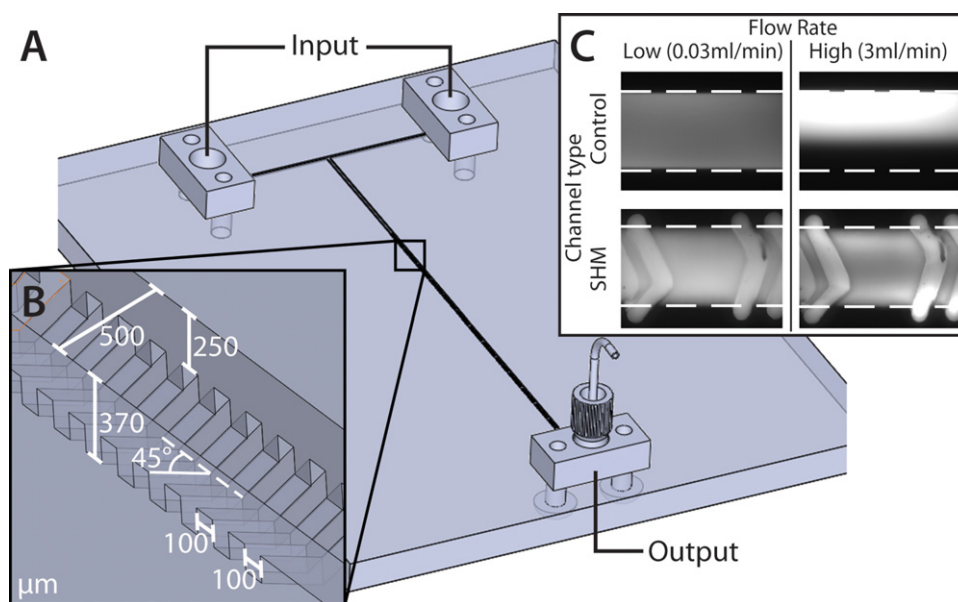


Fig. 1. (A) Exploded view of microfluidic T-junction reactor: channel dimensions are 0.5 mm (w) \times 89.5 mm (l) \times 0.25 mm (d) and the total reactor volume, including tubing is 60 μ L. (B) A staggered herringbone micromixer (SHM) was integrated into the reaction channel. The asymmetric chevron grooves were 100 μ m apart, and set at 45° to the direction of flow. (C) Fluorescein-tagged bovine serum albumin (BSA, 0.3 mg mL⁻¹) was used to illustrate the effectiveness of SHM reactor compared with a control (straight) channel of the same size.

However, in the absence of turbulent fluid flow, mixing in microfluidic reactors is diffusion limited, which can be problematic when dealing with large protein molecules with low diffusivities. To overcome this, passive mixing structures based on a modified version of Stroock's [37] "staggered herringbone micromixer" (SHM), described by Ansari and Kim [38] were machined into the "floor" of the channel. The dimensions of these asymmetric chevron grooves, set at 45° to the direction of flow, were 100 μ m (l) \times 120 μ m (d), across the full width of the channel (500 μ m), arranged in 7 \times 10 cycles (Fig. 1B).

To demonstrate the efficiency of mixing in our microreactor when large protein molecules are involved, T-channel reactors of identical size were fabricated, with and without passive mixing structures. Flow visualisation was carried out with two input solutions: reverse osmosis purified water and a solution of fluorescein-conjugated bovine serum albumin (BSA, 0.3 mg mL⁻¹). These two solutions were run through the inlets at various flow rates, and images were taken at the mid-point of the reactor channel, 4.5 cm from the T-junction (Fig. 1C).

At higher flow rates (1.5–3 mL min⁻¹), at the mid-point of the channel, there was a distinct boundary between the labelled and non-labelled fluid streams in the non-SHM channel, whilst the streams in the SHM channel appear to be completely mixed. At lower flow rates (0.03–0.3 mL min⁻¹) the two streams appeared to be well mixed in both of the reactors, with or without SHM structures, the residence times (at this point of the channel) being sufficiently long to allow diffusion of the protein across the width of the channel. The mixing in the SHM reactor was further characterised with confocal microscopy (see ESI 2).

From these results, one could conclude that the SHM might not be necessary, at least for 'slow' reaction systems where longer residence times (and thus lower flow rates) are required to achieve complete conversion. However, co-flowing enzyme and substrate into a microfluidic channel without rapid and induced mixing will initially lead to partially mixed and unmixed zones [39]. It will be difficult therefore to judge where the two solutions are intermixed enough to form the 'final' concentrations for the reaction and hence impossible to accurately measure the effective residence time. A lack of SHM structures would also

prevent the use of faster flow rates in the reactor, reducing its versatility.

3.1.2. Filtration device

The filtration device was designed to seal membranes in place by clamping, rather than bonding, in order to allow the integration of any membrane type (regardless of material) and so maximise the flexibility of the system. The device consisted of two PMMA plates, both with a straight channel (width 1 mm, depth 1 mm, length 45 mm) and two 1 mm holes milled through at either end to allow fluidic connection (Fig. 2A–C). A recess (1 mm wide, 0.75 mm deep) around the channel on one plate held a PDMS gasket in place, and the filter membrane sat in the resulting enclosure. The plates were clamped together by means of M3 screws along the edges, creating a reversible seal around the membrane that did not require the use of adhesives. In this way, the filter could be quickly repurposed to other applications. This, combined with the standardised interconnects used on both the filter and the reactor, allows the system to be reconfigured to test different process conditions.

To characterise the burst pressure of the filtration unit, the ports on the permeate side of the membrane were capped off, whilst air was pumped into the retentate side with a gas-tight syringe (Fig. 2D). Pressure was logged with a pressure sensor, and showed steady increases with increasing volume of air pumped into the system; a sudden pressure drop indicated the bursting point (Fig. 3A). Burst pressures varied with the torque applied to the screws on both the main assembly and the ports, but somewhat counter-intuitively, higher applied torques resulted in lower burst pressures. This may be due to deformation of the rigid frames of the assembly, leading to poor contact between the frame and the PDMS gasket.

Control of back pressure on the retentate output was achieved by constricting fluid flow in capillaries of specific length and diameter. Capillaries with lengths of 30 cm and internal diameters of 50, 75, 100 and 200 μ m (Upchurch) were connected to the output of the retentate channel, purified water (reverse osmosis) was run through both the retentate and permeate channels at various flow rates, and the back pressure recorded using a pressure sensor

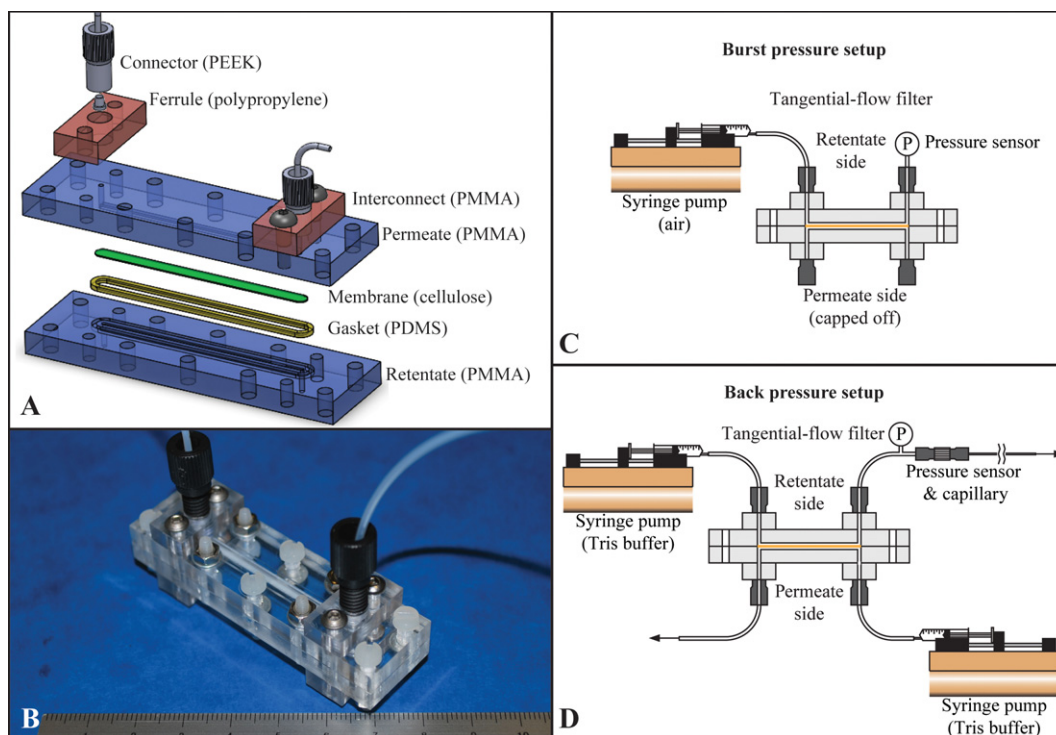


Fig. 2. (A) Exploded view of tangential-flow filter – a membrane fits inside the space created by the gasket and is sealed in place when permeate/retentate plates are clamped together. This ‘clamp and play’ principle does not rely on adhesives, and allows the testing of different membrane types. Additionally, the filter uses the same interconnects as the reactor, allowing the reactor/filter system to be easily reconfigured to test different process conditions; (B) photograph of assembled filter after assembly with M3 screws; (C) schematic of setup used to evaluate the robustness of the sealed filter under pressure; (D) schematic of setup used to measure the effect of outlet capillary dimension on back pressures.

(Honeywell, NJ, USA) with a LabView interface (National Instruments, TX, USA).

It was found that using capillary diameters of 50 μm gave the highest permeate yield at the operating flow rates required by the reactor. At flow rates of 10–30 $\mu\text{L min}^{-1}$, with capillary diameters of 50, 75, 100 and 200 μm , the pressures achieved were in the range of 1–15 psi (Fig. 3B). Back pressure was found to increase linearly with increasing flow rate, and with decreasing capillary diameter. Overall, control of back pressure with capillaries was found to be more reproducible than with commercially available micro-metering valves, with the added advantages of being considerably cheaper, and having no moving parts.

3.2. Transketolase reactions

In order to demonstrate the general applicability of the microfluidic reactor for biocatalysis, two model TK reactions were studied: the wild-type TK-catalysed reaction of hydroxypyruvate (HPA) with glycolaldehyde (GA), and the mutant D469T TK-catalysed reaction of HPA with propanal. Using HPA as a substrate produces carbon dioxide as a by-product, which drives the reaction to completion. The reaction profiles from the batch (96-well plate) and the microfluidic reactors are shown in Fig. 4.

Under standard conditions, the erythrose batch reaction was found to go to completion in approximately 120 min (Fig. 4A). Reaction data were quantified from the calibration curves derived from standard solutions of purified erythrose, and concentrations were measured and found to be at 50 mM, within the margins of error. The time to full conversion is comparable to the work of Matosevic et al. [16]. There was good mass balance between the initial HPA concentration, and the sum of HPA depletion and erythrose formation throughout, and the enantiomeric excess (e.e.) was 90%. The corresponding microfluidic reaction was not

significantly different in conversion time or e.e. (87%). Data are accurate to $\pm 4\%$.

Similar to the HPA reaction with GA, the reaction of HPA with propanal (Fig. 4B), catalysed by the mutant TK, showed no significant difference between the batch and microfluidic reaction rates (these were faster than the erythrose reaction, approaching completion after 60 min). Enantiomeric excess values of 66% and 65% ($\pm 4\%$) were determined for the DHP product in the batch and microfluidic reactors respectively, consistent with earlier reports [26,33].

Since the mode of enzyme/substrate interaction is solution-based for both the batch and continuous flow reactors, we would expect similar reaction rates and e.e. data for each system.

Microwell platforms such as 96-well plates are standard equipment for the study of bioprocesses, offering rapid data generation and process optimisation [40]. However, the continuous operation of the microfluidic system allows us to move beyond probing and optimising reaction conditions and switch to small-scale production without further changes to our experimental set-up. At conditions where 100% conversion is achieved, the microreactor is capable of producing 0.72 mg h^{-1} of erythrose, or 0.36 mg h^{-1} DHP.

Previous work on enzymatic microfluidic reactors has tended to focus on supported enzymes [3,7,16–18,41]. Although these examples show reduced enzyme activity and may involve complicated immobilisation techniques, they are favoured because there is less risk of clogging microchannels with cell debris. We found that the use of partial clarification techniques, where the crude lysate was centrifuged to spin out the cell debris and the supernatant separated off and filtered, gave solutions with high enzymatic activity which did not clog the channels.

Synthetic pathways of many high-value compounds involve multiple steps. The full conversion (without the need for recirculation) observed in the microfluidic reactor is of great

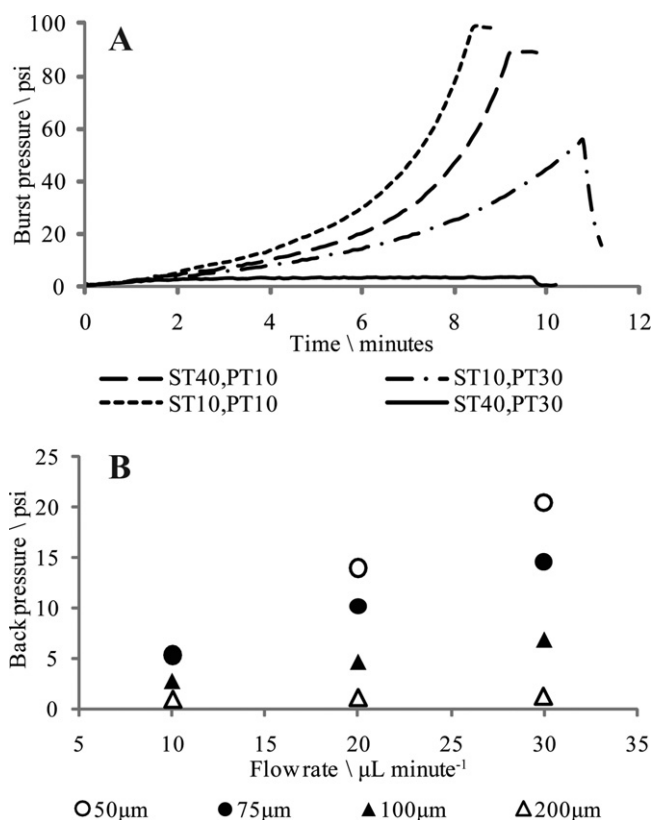


Fig. 3. (A) To test the sealing strength of the ‘clamp and play’ principle, the filtration unit was assembled with various screw torques (ST = torque on main assembly screws; PT = port attachment screws; units are Ncm for both). Pressure profiles were generated by pumping air into the unit using the burst pressure set-up shown in Fig. 2C. Sudden drop of pressure indicates burst pressure; (B) to generate the back pressure necessary for optimum permeate yield, capillaries of various inner diameters were connected to the filtration unit (cf. Fig. 2D) and analysed for back pressure at various flow rates.

significance, as the product of one reactor may become a continuous source of a required substrate for another, when integrated into a larger modular platform.

3.3. Filtration experiments, “model reactor output”

If we wish to connect reactor modules in series for a multi-step reaction, it is desirable to have a purification step for the product of the first reactor before it enters the next one. To this end, an inline tangential flow filtration was investigated, using erythrose and lysate solutions designed to mimic the expected output from the reactor. SDS-PAGE studies from a representative selection of flow conditions confirmed that a membrane with 10 kDa molecular weight cut-off was sufficient to ensure the full retention of transketolase along with all other protein in the lysate (Fig. 5). Similar concentrations of L-erythrose were found in the permeate and retentate solutions (as measured by HPLC), indicating that the compound is able to permeate the membrane freely, without adsorption or other interactions.

To improve the yield of the product, therefore, it is essential that the volume of permeate fluid is maximised, which can be done by increasing the back pressure on the retentate outlet, forcing more fluid across the membrane. To investigate this, 30 cm capillaries with internal diameters of 100 μm, 75 μm and 50 μm were connected to the retentate outlet, and the permeate and retentate volume outputs measured under various flow conditions (Table 1).

Interestingly, increasing the flow rate from 10 to 30 μL min⁻¹ had little effect on the permeate yield for any given capillary, but

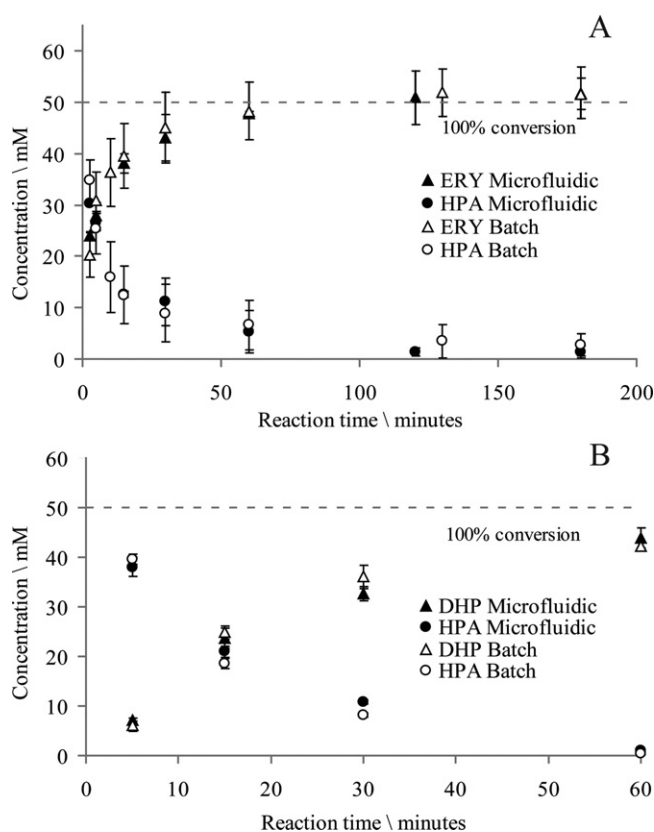


Fig. 4. (A) Reaction profiles in batch and microfluidic reactors for the TK-catalysed reaction of HPA (● = microfluidic, ○ = batch reactor) with GA to produce L-erythrose (ERY, ▲ = microfluidic, △ = batch). Reaction conditions: 50 mM HPA, 50 mM GA, 0.34 mg mL⁻¹ *E. coli* TK wild type, 2.4 mM thiamine diphosphate (ThDP), 9.8 mM MgCl₂, room temperature, pH 7. Batch data show average of two experiments run in triplicate (error bars are half-min/max of the two averages), microfluidic data is from a single experiment run in triplicate (error bars are standard deviation). (B) Reaction profiles for mutant TK-catalysed reaction of HPA (● = microfluidic, ○ = batch reactor) with propanal to produce DHP (▲ = microfluidic, △ = batch). Reaction conditions: 50 mM HPA, 70 mM propanal, 0.33 mg mL⁻¹ *E. coli* transketolase mutant D469T, 2.4 mM ThDP, 9.8 mM MgCl₂, room temperature, pH 7. Error bars represent standard deviation from three experiments.

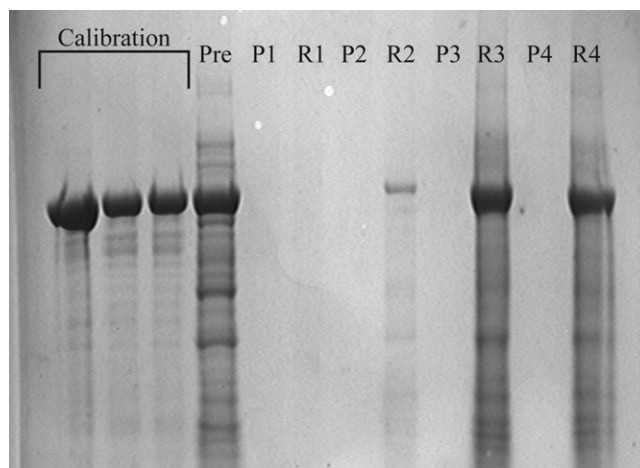


Fig. 5. SDS-PAGE of samples taken before and after filtration. The samples from the permeate stream (P1, P2, P3) show no proteins present, implying that the TK is completely retained by the filter. Pre = pre-filtration sample, R = retentate sample, and P = permeate sample. Total input to filter was calculated at 15.2 mg, output from retentate 11.7 mg.

Table 1

Comparison of permeate volumetric output as a percentage of the total filter output, and the back pressures generated, under various conditions of capillary diameter and flow rate.

Capillary diameter/ μm		Flow rate/ $\mu\text{L min}^{-1}$		
		10	20	30
50	% permeate (pressure/psi)	89(5.3)	56 (14)	67 (20)
75	% permeate (pressure/psi)	85(5.3)	41 (10)	36 (15)
100	% permeate (pressure/psi)	31 (2.7)	24(4.6)	25(6.9)

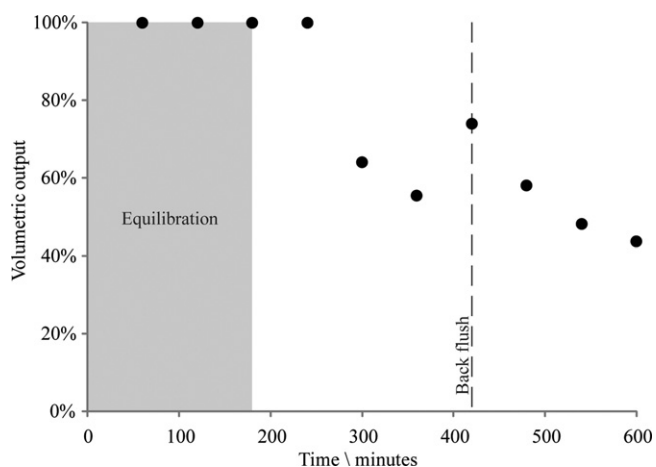


Fig. 6. Permeate output as a percentage of the total from a filtration unit connected to an enzymatic reactor for long-term continuous production of L-erythrulose. A back-flush of the membrane with purified water at 420 min partially restored the permeate yield.

the yield notably improved as capillaries with decreasing internal diameter were used, regardless of the flow rate operated. It is possible that although an increased flow rate would increase the back pressure, and thus the permeate yield, under these conditions more material would be pushed into the membrane and fouling would be increased, negating any increase in the driving force.

Optimum conditions were found to hold with a 50 μm capillary, operating at a flow rate of 10 $\mu\text{L min}^{-1}$; this gave a permeate yield of 95%, and the flow rate was compatible with an optimal residence time for an upstream microfluidic reactor.

3.4. Integration of microfluidic reactor with filtration device

In order to investigate the continuous synthesis of erythrulose with our system, the output of the microfluidic enzymatic reactor was connected in series with a filtration unit and run for 10 h. Conditions had been optimised for the reactor, with GA and HPA concentrations of 50 mM, 3 mg mL^{-1} TK, and a flow rate of 10 $\mu\text{L min}^{-1}$, corresponding to a residence time of 120 min. A capillary of 50 μm diameter was fitted to the retentate outlet to maximise the permeate yield.

HPLC analysis showed that complete conversion of the GA and HPA to erythrulose occurred throughout the experiment – there was no loss of activity of the TK. The yield of erythrulose recovery was therefore entirely dependant on the partition of fluid between the permeate and retentate. It was found (Fig. 6) that the permeate output was stable at almost 100% for 2 h (once the remaining Tris required for the priming of the system had been flushed out), after which it declined sharply, presumably due to build-up of lysate material on surface of membrane, reducing the permeability and therefore the flux. After 7 h, the filtration unit was back-washed with purified water in an attempt to remove this material, and the permeate yield was restored to 70–80%.

The long-term performance of the filter could be improved in several ways. Modifying the reaction conditions to reduce the residence time (for example, by increasing TK concentration) would also reduce the amount of time required to prime (and equilibrate) the system, thereby minimising the material lost during this stage of the process. The filter itself could be also modified to improve the surface area available for product transmission. Finally, the back-washing process could be incorporated into the system and automated with the help of electronically actuated valves and pumps to reduce the build-up of cellular debris on the membrane surface.

4. Conclusion

In this work we have successfully demonstrated the use of a modular continuous flow microfluidic reactor with in-line separation of the biocatalyst for the transketolase-catalysed coupling of the irreversible donor hydroxypyruvate to the acceptors glycolaldehyde and propanal. Complete or nearly complete conversion has been achieved rapidly in the microfluidic reactor for two model reaction systems which use substrates of different hydrophobic properties. The rate of conversion to product is comparable to batch reactors, thus facilitating high-throughput evaluation of biocatalytic process conditions and rapid process development. In addition, the reaction times can be shortened by increasing the activities of the biocatalysts utilised.

This is especially interesting for the design and reaction development of biocatalytic carbon–carbon bond formation systems with labile substrates or products [30,32,42] leading to unwanted non-enzymatic side-reactions.

We also report the complete separation of the transketolase enzyme from the product stream by means of a tangential flow filtration device, affording yields of approximately 65%. These yields could be improved by relatively simple modifications to the reaction conditions and the design of the system.

With significant advances in bioreactor miniaturisation made, the next logical step for micro-scale bioprocessing is the integration of downstream unit operations [43]. Whilst such efforts have been made in batch reactors, there has been little work on the development of equivalent microfluidic systems. We believe that our integration of a microreactor for synthesis and in-line downstream processing on a microfluidic platform is a significant step towards the modular cascading of reaction and separation units, and thus towards the realisation of complete “lab on chip” devices for the development of whole biocatalytic processes [44,45]. The modular aspect of the system facilitates the easy integration of new features, in particular analytical devices, which are increasingly important in microfluidic bioprocess development [46]. It also opens new operational opportunities for laboratory-scale development and production of a number of metabolites. The system could be used to rapidly optimise operational conditions (for example, enzyme concentration) to make industrial synthesis processes more economically viable. Furthermore, beyond the simple transfer of unit operations from conventional to microfluidic formats, this development is also of interest to solve fundamental challenges in

the molecular and engineering aspects of interfacing two and more reaction steps, which would be incompatible in the same reaction compartment, for the important biocatalytic multi-step synthesis of metabolites [47].

Acknowledgements

The authors would like to acknowledge the BBSRC, EPSRC and CONACYT for providing funding for studentships to James Lawrence, Homam Al-Bahrani and Armando Cázares respectively. The authors would also like to thank David Steadman for his help in purifying L-erythrulose for HPLC standards and Marcel Reichen for his support on fabrication.

Appendix A. Supplementary data

Supplementary data associated with this article can be found, in the online version, at doi:10.1016/j.molcatb.2011.12.010.

References

- [1] C. Wiles, P. Watts, *Eur. J. Org. Chem.* 10 (2008) 1655–1671.
- [2] P.L. Urban, D.M. Goodall, N.C. Bruce, *Biotechnol. Adv.* 24 (2006) 42–57.
- [3] M.S. Thomsen, P. Polt, B. Nidetzky, *Chem. Commun.* 24 (2007) 2527–2529.
- [4] M. Tišma, B. Zelić, Đ. Vasić-Rački, P. Žnidaršič-Plazl, I. Plazl, *Chem. Eng. J.* 149 (2009) 383–388.
- [5] P. He, G. Greenway, S.J. Haswell, *Process Biochem.* 45 (2010) 593–597.
- [6] H.R. Luckarift, B.S. Ku, J.S. Dordick, J.C. Spain, *Biotechnol. Bioeng.* 98 (2007) 701–705.
- [7] B. Ngamsom, A.M. Hickey, G.M. Greenway, J.A. Littlechild, P. Watts, C. Wiles, *J. Mol. Catal. B: Enzym.* 63 (2010) 81–86.
- [8] M.N.H.Z. Alam, M. Pinelo, K. Samanta, G. Jonsson, A. Meyer, K.V. Gernaey, *Chem. Eng. J.* 167 (2011) 418–426.
- [9] K. Koch, R.J.F. van den Berg, P.J. Nieuwland, R. Wijtmans, H.E. Schoemaker, J.C.M. van Hest, F.P.J.T. Rutjes, *Biotechnol. Bioeng.* 99 (2008) 1028–1033.
- [10] M. Miyazaki, H. Maeda, *Trends Biotechnol.* 24 (2006) 463–470.
- [11] H.R. Sahoo, J.G. Kralj, K.F. Jensen, *Angew. Chem. Int. Ed.* 119 (2007) 5806–5810.
- [12] R.L. Hartman, J.R. Naber, S.L. Buchwald, K.F. Jensen, *Angew. Chem. Int. Ed.* 49 (2010) 899–903.
- [13] R. Wohlgenuth, *Chem. Biochem. Eng. Q.* 25 (2011) 125–134.
- [14] R. Wohlgenuth, in: M. Moo-Young, M. Butler, C. Webb, A. Moreira, B. Grodzinski, Z.F. Cui, S. Agathos (Eds.), *Comprehensive Biotechnology*, Elsevier, Amsterdam, Netherlands, 2011, pp. 591–601.
- [15] A. Schwarz, M.S. Thomsen, B. Nidetzky, *Biotechnol. Bioeng.* 103 (2009) 865–872.
- [16] S. Matosevic, G.J. Lye, F. Baganz, *Biotechnol. Prog.* 26 (2010) 118–126.
- [17] K.F. Schilke, K.L. Wilson, T. Cantrell, G. Corti, D.N. McIlroy, C. Kelly, *Biotechnol. Prog.* 26 (2010) 1597–1605.
- [18] R. Moser, T. Chappuis, E. Vannioli, S. Crefier, O. Naef, *Chimia* 64 (2010) 799–802.
- [19] M.A. Holden, S.Y. Jung, P.S. Cremer, *Anal. Chem.* 76 (2004) 1838–1843.
- [20] A. Srinivasan, H. Bach, D.H. Sherman, J.S. Dordick, *Biotechnol. Bioeng.* 88 (2004) 528–535.
- [21] R. van Reis, A. Zydney, *J. Membr. Sci.* 297 (2007) 16–50.
- [22] J. de Jong, R.G.H. Lammertink, M. Wessling, *Lab Chip* 6 (2006) 1125–1139.
- [23] M. Kalyanpur, *Mol. Biotechnol.* 22 (2002) 87–98.
- [24] I.S. Ngene, R.G.H. Lammertink, M. Wessling, W. van der Meer, *J. Membr. Sci.* 346 (2010) 202–207.
- [25] R. Wohlgenuth, M.E.B. Smith, P.A. Dalby, J.M. Woodley, in: M.C. Flickinger (Ed.), *Encyclopaedia of Industrial Biotechnology: Bioprocess, Bioseparation and Cell Technology*, Wiley, Hoboken, USA, 2010, pp. 4746–4752.
- [26] A. Cázares, J.L. Galman, L.G. Crago, M.E.B. Smith, J. Strafford, L. Ríos-Solis, G.J. Lye, P.A. Dalby, H.C. Hailes, *Org. Biomol. Chem.* 8 (2010) 1301–1309.
- [27] E.G. Hibbert, T. Senussi, S.J. Costelloe, W. Lei, M.E.B. Smith, J.M. Ward, H.C. Hailes, P.A. Dalby, *J. Biotechnol.* 131 (2007) 425–432.
- [28] E.G. Hibbert, T. Senussi, M.E.B. Smith, S.J. Costelloe, J.M. Ward, H.C. Hailes, P.A. Dalby, *J. Biotechnol.* 134 (2008) 240–245.
- [29] F. Charmantray, V. Heïlaine, B. Legeret, L. Hecquet, *J. Mol. Catal. B: Enzym.* 57 (2009) 6–9.
- [30] R. Wohlgenuth, *J. Mol. Catal. B: Enzym.* 61 (2009) 23–29.
- [31] C.U. Ingram, M. Bommer, M.E.B. Smith, P.A. Dalby, J.M. Ward, H.C. Hailes, G.J. Lye, *Biotechnol. Bioeng.* 96 (2007) 559–569.
- [32] J. Shaeri, I. Wright, E. Rathbone, R. Wohlgenuth, J.M. Woodley, *Biotechnol. Bioeng.* 101 (2008) 761–767.
- [33] M.E.B. Smith, E.G. Hibbert, A.B. Jones, P.A. Dalby, H.C. Hailes, *Adv. Synth. Catal.* 350 (2008) 2631–2638.
- [34] M.E.B. Smith, K. Smithies, T. Senussi, P.A. Dalby, H.C. Hailes, *Eur. J. Org. Chem.* 5 (2006) 1121–1123.
- [35] S. Matosevic, M. Micheletti, J.M. Woodley, G. Lye, F. Baganz, *Biotechnol. Lett.* 30 (2008) 995–1000.
- [36] H.A. Stone, A.D. Stroock, A. Ajdari, *Annu. Rev. Fluid Mech.* 36 (2004) 381–411.
- [37] A.D. Stroock, S.K.W. Dertinger, A. Ajdari, I. Mezic, H.A. Stone, G.M. Whitesides, *Science* 295 (2002) 647–651.
- [38] M.A. Ansari, K.Y. Kim, *Chem. Eng. Sci.* 62 (2007) 6687–6695.
- [39] W.D. Ristenpart, J. Wan, H.A. Stone, *Anal. Chem.* 80 (2008) 3270–3276.
- [40] G.J. Lye, P. Ayazi-Shamlou, F. Baganz, P.A. Dalby, J.M. Woodley, *Trends Biotechnol.* 21 (2003) 29–37.
- [41] M.B. Kerby, R.S. Legge, A. Tripathi, *Anal. Chem.* 78 (2006) 8273–8280.
- [42] J. Shaeri, R. Wohlgenuth, J.M. Woodley, *Org. Proc. Res. Dev.* 10 (2006) 605–610.
- [43] M.P.C. Marques, J.M.S. Cabral, P. Fernandes, *Recent Pat. Biotechnol.* 3 (2009) 124–140.
- [44] G.M. Whitesides, *Nature* 442 (2006) 368–373.
- [45] A.J. DeMello, *Nature* 442 (2006) 394–402.
- [46] J.M. Bolivar, J. Wiesbauer, B. Nidetzky, *Trends Biotechnol.* 29 (2011) 333–342.
- [47] R. Wohlgenuth, *Biotechnol. J.* 4 (2009) 1253–1265.